

## Transport Characterization of the Magnetic Anisotropy of (Ga,Mn)As

K. Pappert, S. Humpfer, J. Wenzsch, K. Brunner, C. Gould, G. Schmidt, and L. W. Molenkamp  
 Physikalisches Institut (EP3), Universität Würzburg, Am Hubland, D-97074 Würzburg, Germany  
 (dated: March 23, 2024)

The rich magnetic anisotropy of compressively strained (Ga,Mn)As has attracted great interest recently. Here we discuss a sensitive method to visualize and quantify the individual components of the magnetic anisotropy using transport. A set of high resolution transport measurements is compiled into color coded resistance polar plots, which constitute a fingerprint of the symmetry components of the anisotropy. As a demonstration of the sensitivity of the method, we show that these typically reveal the presence of both the  $\bar{[110]}$  and the  $[010]$  uniaxial magnetic anisotropy component in (Ga,Mn)As layers, even when most other techniques reveal only one of these components.

The ferromagnetic semiconductor (Ga,Mn)As exhibits rich magnetic anisotropy behaviour. Experimental studies of compressively strained (Ga,Mn)As based on direct magnetization measurements by SQUID magnetometry [1] show a principally biaxial anisotropy in the sample plane for highly doped samples at 4 K. Additionally, uniaxial anisotropy components along  $\bar{[110]}$  [2] or  $[010]$  [3] have been reported. The  $\bar{[110]}$  uniaxial anisotropy is widely accepted to be present in most (Ga,Mn)As layers as a secondary component at 4 K which gets stronger upon annealing, or increasing sample temperature. The primary biaxial anisotropy is expected from theory [4, 5] and originates from the hole-mediated ferromagnetism and the strong spin orbit coupling, which links the magnetic interactions to the lattice structure. This theory also provides a partial understanding of the emergence of a different easy axis for higher carrier concentration or temperature, in that it predicts a transition from biaxial along  $h100i$  to biaxial along  $h110i$ . It does not however account for the presence of either uniaxial term. Nevertheless, the existence of these uniaxial easy axes is experimentally well established, and it remains of great interest, both as a practical matter in designing and controlling magnetization in experimental samples and as a fundamental tool for increasing our understanding of the magnetization behaviour in strong spin-orbit systems, to develop tools to precisely investigate the magnetic anisotropy in (Ga,Mn)As.

Traditionally the anisotropy in these materials has been investigated by direct measurement of the projection of the magnetization onto characteristic directions using SQUID or VSM. The advent of vector field magnets has recently opened up new possibilities for acquiring a detailed mapping of the anisotropy. We present one such method here, based on summarizing the results of transport measurements into color coded resistance polar plots (RPP) which act as fingerprints for the anisotropy of a given structure. Not only is this method faster than the traditional alternatives, but it is also more sensitive to certain secondary components of the anisotropy, in particular those with easy axes collinear to the primary anisotropy [6]. The technique thus often reveals the exis-

tence of components which would be missed using standard techniques. Moreover, the technique can be applied to study the anisotropy of layers by using macroscopic transport structures, or applied directly to device elements. It can thus reveal any impacts of processing or the influence of small strain fields due to, for example, contacting.

Here, we apply the RPP technique to verify that both the  $[010]$  and the  $\bar{[110]}$  uniaxial anisotropy terms can be, and typically are, simultaneously present in compressively strained (Ga,Mn)As layers at 4 K. Color coded polar plots can be compiled from any measurement data that shows a response to the magnetization direction. Anisotropic magnetoresistance (AMR) [7], tunneling anisotropic magnetoresistance (TAMR) [3] or in-plane Hall (IPH) measurements [2] are typical examples in (Ga,Mn)As. For example, sending a current  $J$  through a (Ga,Mn)As Hall bar device along  $\# = 0$ , yields a  $\sin(2\#)$ -dependence of the transverse resistance  $R_{xy}$  on the magnetization direction  $\#$  due to the IPH effect [7]:  $R_{xy}(\#) = (R_{xy}) \sin(2\#)$

We demonstrate the usefulness of the technique by applying it to the characterization of a typical 20 nm thick (Ga,Mn)As layer grown on a GaAs (001) substrate by low-temperature molecular beam epitaxy. It is patterned into a 60  $\mu$ m wide Hall bar oriented along the  $h110i$  crystal direction by optical lithography and chlorine assisted dry etching. Contacts are established through metal evaporation and lift off.

Transport measurements are carried out in a magnetocryostat fitted with a vector field magnet comprised of three mutually orthogonal pairs of Helmholtz coils that allow the application of a magnetic field of up to 300 mT in any direction. An angular set of IPH curves is acquired while sweeping the magnetic field along multiple directions in the sample plane. For each individual angle the magnetization state of the sample is first prepared by a strong negative magnetic field along  $\hat{z}$ . The field is then slowly brought down to zero while assuring that the field vector never deviates from the  $\hat{z}$  direction. The IPH curve as a function of positive magnetic field in the  $\hat{z}$  direction is then acquired from zero to higher fields,

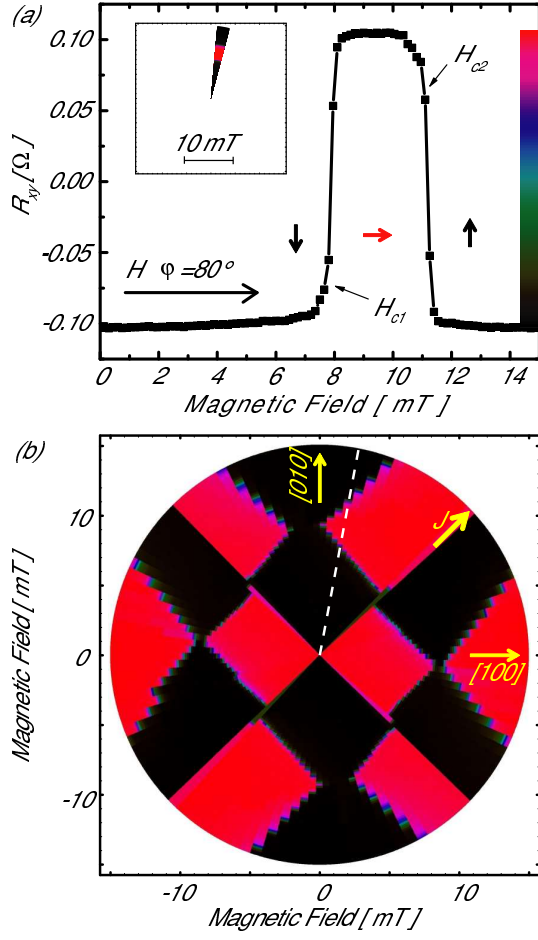


FIG. 1: (a) In-plane Hall measurement along  $\varphi = 80^\circ$  with marked first and second switching field, color scale and the corresponding section of a color coded resistance polar plot (inset). (b) Resistance polar plot from a full set of in-plane Hall measurements along every  $3^\circ$ . The  $80^\circ$ -section corresponding to (a) is marked by a dashed line.

and these results are displayed in a RPP as in Fig. 1b.

Fig. 1a shows a typical IPH measurement. After magnetizing the sample along  $80^\circ$  at  $\sim 300$  mT, the magnetization relaxes towards the  $[010]$  easy axis, as the field is brought back to zero. This corresponds to the negative resistance state associated with an angle of  $\theta = 135^\circ$  between  $\mathbf{J}$  and  $\mathbf{M}$ . The first abrupt resistance change at the field  $H_{c1}$  corresponds to a  $90^\circ$  reorientation of  $\mathbf{M}$  towards the other (GaMn)As easy axis  $[001]$ . A second reorientation of  $\mathbf{M}$  towards  $[010]$  at  $H_{c2}$  completes the magnetisation reversal. A set of such magnetic field scans along many angles, here every  $3^\circ$ , is compiled into a RPP with the magnetic field  $H$  along the radius and each scan at its angle  $\varphi$ .

The inset of Fig. 1a shows the  $80^\circ$ -segment of the full RPP of Fig. 1b. The intensity encodes the normalized resistance value, where low and high denote the minimum and maximum resistance of the entire curve set, respectively. The positions of the switching fields in the polar

plot and the symmetry of the pattern they form contain information on the underlying magnetic anisotropy.

We now explain the observed pattern and the conclusions that we may infer from it. As already noted, (GaMn)As layers grown on a GaAs (001) substrate are compressively strained and exhibit a biaxial magnetic anisotropy ( $K_1$ ) with the two easy axes along  $[100]$  and  $[010]$  at 4 K. Additional smaller uniaxial anisotropy components collinear to one of the biaxial easy axes, for example  $[010]$  ( $K_{u1}$ ) [3] or bisecting the biaxial easy axes, along  $[\bar{1}10]$  ( $K_{u2}$ ) [2] have been previously reported. The energy  $E$  of a single (GaMn)As domain with magnetization  $\mathbf{M}$  pointing in  $\theta$ - and external magnetic field  $H$  in  $\varphi$ -direction is thus phenomenologically expressed as:

$$E = \frac{K_1}{4} \sin^2(2\theta) + K_{u1} \sin^2(\theta) + K_{u2} \sin^2(\theta - 45^\circ) - M H \cos(\theta - \varphi) \quad (1)$$

where the last term is the Zeeman energy. When an external magnetic field is applied, the magnetization direction follows a local energy minimum (coherent or Stoner-Wohlfarth rotation). However, if the energy gained by a magnetization reorientation to any other energy minimum is larger than the respective domain wall (DW) nucleation/propagation energy  $\epsilon$ , a DW is nucleated and propagates through the structure, resulting in an abrupt magnetization reversal. Due to the mainly biaxial nature of the magnetic anisotropy the magnetization typically reverses in a double-step switching process through the nucleation and propagation of two  $90^\circ$  DW, as in Fig. 1a.

We first discuss the regime, where DW nucleation/propagation dominates the magnetization reversal process, i.e. where  $\epsilon$  is much smaller than the crystalline anisotropy. We start with the pure biaxial magnetic anisotropy, i.e., with  $K_{u1} = K_{u2} = 0$ . During the double-step switching process, the magnetostatic energy minima remain to a good approximation along the biaxial easy axes, whose difference in energy is given by the Zeeman term in Eq. 1. When the energy gained through a  $90^\circ$  magnetization reorientation is larger than  $\epsilon_{90}$ , the nucleation and propagation energy of a  $90^\circ$ -DW, a thermally activated switching event becomes possible, which on the timescale of our measurement, results in an immediate switching event. The polar plot in Fig. 2a shows the characteristic square pattern formed by these switching fields [6], Fig. 2b the corresponding calculated RPP. The switching field positions (thick black lines) can be expressed in cartesian coordinates ( $x = H_c \cos \varphi$ ;  $y = H_c \sin \varphi$ ) as given in Tab. I. The diagonals (grey) of the  $H_{c1}$ -square represent the biaxial easy axes of the material (here along  $0^\circ$  and  $90^\circ$ ). The diagonal's length is equal to  $\frac{2\epsilon_{90}}{M}$ . The dashed lines represent the hard magnetic axes. The arrows illustrate the direction of the magnetization and their color the corresponding resistance state of the respective section.

An additional small uniaxial anisotropy  $K_{u1}$  along one

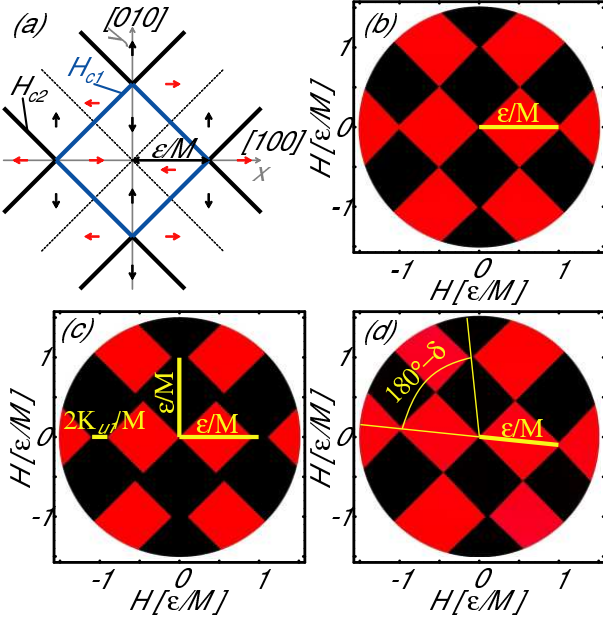


FIG. 2: (a) Switching field positions (thick solid lines) in a polar plot for a biaxial material with easy axes along [100] and [010] (gray). The magnetization direction in each region of the plot is indicated by arrows (red/black: high/low resistance) and the hard axes by dashed lines. (b-d) Simulated resistance polar plots for a biaxial material with easy axes along the [100] and [010] crystal directions (b) and the same material with an additional uniaxial anisotropy along [010] (c) or [110] (d). Color scale of the resistance as in Fig. 1.  $\theta$  denotes the 90° DW nucleation/propagation energy.

Anisotropy components	$H_c$ -positions in polar plot
h100i	$y = x \cdot \frac{\mu}{M}$
h100i + [010]	$y = x \cdot \frac{\mu}{M} \cdot \frac{K_{u1}}{M}$
h100i + [110]	$y = \begin{cases} +x \cdot \frac{\mu}{2M} \cos(45^\circ - \theta) \\ x \cdot \frac{\mu}{2M} \cos(45^\circ + \theta) \end{cases}$

TABLE I: Positions of the switching fields in a polar plot given in cartesian coordinates ( $x = H_c \cos \theta$ ;  $y = H_c \sin \theta$ ).  $\theta = 2$  is the angle between global and biaxial easy axis as in Fig. 2d (see text).

of the biaxial easy axes (here along 90°) alters this pattern as shown in Fig. 2c. The symmetry between the two biaxial easy axes is lifted, since one of them is parallel ( $B_e U_e$ ) and one perpendicular ( $B_e U_h$ ) to the easy axis of the uniaxial component. The switching field positions in Tab. I can be derived as discussed above [6]. 90°-switches away from (towards) the  $B_e U_e$  axis occur now at higher (lower) magnetic fields as compared to the pure biaxial anisotropy. Typical steps in the  $H_{c1}$ -pattern emerge (Fig. 2c, e.g. along 45°). The strength of the uniaxial anisotropy can be determined from the separation  $\frac{2K_{u1}}{M}$  between  $H_{c1}$  and  $H_{c2}$  along the  $B_e U_h$  axis. A further characteristic feature is the "open corner"

of the  $H_{c1}$ -pattern along the  $B_e U_e$  axis. A 180° magnetization reversal becomes energetically more favorable in this angular region, than two successive 90° events [6, 8]. Since the isotropic magnetoresistance of typical samples is relatively small, two magnetization directions differing by 180° are not distinguishable on the scale considered here, and have the same color in the RPP.

If on the other hand, apart from the main biaxial anisotropy ( $K_1$ , h100i), a uniaxial anisotropy  $K_{u2}$  with easy axis along [110] (here 135°) is also present and assuming that the DW nucleation/propagation energy depends on the angle  $\theta$  between the two domains as  $\theta = \theta_{90} (1 - \cos(\theta))$ , the calculation gives the RPP of Fig. 2d. The uniaxial anisotropy component flattens the energy surface and shifts the positions of the biaxial energy minima by  $\frac{\theta}{2} = \frac{1}{2} \arcsin(\frac{K_{u2}}{K_1})$  towards the uniaxial easy axis [9]. The resulting "global easy axes" appear as diagonals of a characteristic rectangle in the RPP, where the uniaxial easy axis is along the median line of the longer edge. The positions of the switching events (Tab. I) can be derived equating  $\theta$  with the difference in Zeeman energy between the minima. The diagonal's length is again equal to  $\frac{2\theta_{90}}{M}$ .

We demonstrate the usefulness of the technique by applying it to the characterization of the typical (Ga,Mn)As sample discussed in Fig. 1. The RPP in Fig. 1b shows an  $H_{c1}$ -pattern with both an elongation in [110]-direction and steps along the hard axes. Both uniaxial anisotropy components are thus clearly present. From the length of the diagonals we estimate  $\frac{\mu}{M} = 8$  mT. The step height gives  $\frac{K_{u1}}{M} = 1$  mT. From the rectangle side-ratio we obtain  $\theta = 8^\circ$ .  $K_{u2}$  is thus 15% of  $K_1$ .  $\frac{K_1}{M} = 100$  mT can be estimated from the asymptotic behavior of the magnetization towards the hard axes at higher fields and  $M = 37,000$  A/m is known from SQUID measurements.

The anisotropy components and  $\theta$  can differ from sample to sample. Neglecting coherent rotation is typically a good model for the first switching fields  $H_{c1}$ , whereas  $H_{c2}$  is strongly influenced by magnetization rotation especially along the hard axes, as can be seen in Fig. 1b. Sharp switching events are easily identified by high contrast, whereas gradual magnetization rotations show up as smooth color transitions.

In conclusion we have shown that RPP compiled from high resolution IPH measurements constitute a fingerprint of the (Ga,Mn)As anisotropy. They allow both qualitative and quantitative statements about the symmetry components of the magnetic anisotropy and the DW nucleation/propagation energy. The same technique is equally applicable to any transport phenomena which produces a response to the orientation of the magnetization, such as AMR, or TAMR.

We applied the method to several typical MBE layers from our lab [10] to confirm that biaxial and both the [110] and the [010] uniaxial anisotropy terms are

present in all typical compressively strained (Ga,Mn)As layers at 4 K with a relative strength of the order of  $K_{11} : K_{u2} : K_{u1} = 100 : 10 : 1$ . Indeed all (Ga,Mn)As layers investigated show both these uniaxial components, including layers where the [10] component could not be identified in SQUID measurements. Moreover the application of our fingerprint method to previously published data in the literature shows that in all cases where sufficient data is available, both uniaxial components are present.

The authors thank O. Rival and M. Sawicki for useful discussions and V. Hock for sample preparation, and acknowledge financial support from the EU NANO SPIN project (FP6-IST-015728) and the German DFG (BR1960/2-2) project.

- 
- [1] M. Sawicki, F. Matsukura, A. Idziaszek, T. Dietl, G. M. Schott, C. Ruster, C. Gould, G. Karczewski, G. Schmidt, and L. W. Molenkamp, Phys. Rev. B. 70, 245325 (2004).  
 [2] H. X. Tang, R. K. Kawakami, D. D. Awschalom and M. L.

- Roukes Phys. Rev. Lett. 90, 107201 (2003).  
 [3] C. Gould, C. Ruster, T. Jungwirth, E. Girgis, G. M. Schott, R. Giraud, K. Brunner, G. Schmidt, and L. W. Molenkamp Phys. Rev. Lett. 93, 117203 (2004).  
 [4] T. Dietl, H. Ohno and F. Matsukura, Phys. Rev B 63, 195205 (2001).  
 [5] M. Abolfath, T. Jungwirth, J. Brun and A. MacDonald, Phys. Rev. B 63, 054418 (2001).  
 [6] R. P. Cowburn, S. J. Gray, J. Ferre, J. A. C. Bland, J. Miltat, J. Appl. Phys. 78, 7210 (1995)  
 [7] a) T. R. McGuire, R. I. Potter, IEEE Trans. Magn. MAG-11, 1018 (1975). b) J. P. Jan, in "Solid State Physics" (Eds: F. Seitz, D. Turnbull), Academic Press Inc., New York, 1957.  
 [8] Because of the underlying biaxial anisotropy, a 180° DW can be seen as two loosely coupled 90° DW, thus "180° 2"90 [6].  
 [9] C. Daboo, R. J. Hicken, D. E. P.aley, M. Gester, S. J. Gray, A. J. R. Ives, and J. A. C. Bland, J. Appl. Phys. 75, 5586 (1994)  
 [10] Preliminary measurements on samples obtained from other labs have yielded similar results. Final results on these will be published elsewhere.